Talanta 93 (2012) 257–263

Contents lists available at SciVerse ScienceDirect

Talanta

journal homepage: www.elsevier.com/locate/talanta

Growth and properties of Ag-doped ZnO nanoflowers for highly sensitive phenyl hydrazine chemical sensor application

Ahmed A. Ibrahim[a,1], G.N. Dar[b,c,d,1], Shabi Abbas Zaidi[a,b,*], Ahmad Umar[a,b,*], M. Abaker[b,c,d], H. Bouzid[b,c,d], S. Baskoutas[d]

[a] Department of Chemistry, Faculty of Sciences and Arts, Najran University, Najran University, P.O. Box 1988, Najran 11001, Saudi Arabia
[b] Promising Centre for Sensors and Electronic Devices (PCSED), Centre for Advanced Materials and Nano-Research (CAMNR), Najran University, P.O. Box 1988, Najran 11001, Saudi Arabia
[c] Department of Physics, Faculty of Sciences and Arts, Najran University, Najran University, P.O. Box 1988, Najran 11001, Saudi Arabia
[d] Department of Materials Science, University of Patras, Rio Patras GR-26504, Greece

ARTICLE INFO

Article history:
Received 27 December 2011
Received in revised form 11 February 2012
Accepted 15 February 2012
Available online 22 February 2012

Keywords:
Ag-doped ZnO nanoflowers
Structural and optical properties
Phenyl hydrazine chemical sensor

ABSTRACT

We report here the fabrication of a robust, highly sensitive, reliable and reproducible phenyl hydrazine chemical sensor using Ag-doped ZnO nanoflowers as efficient electron mediators. The Ag-doped ZnO nanoflowers were synthesized by facile hydrothermal process at low-temperature and characterized in detail in terms of their morphological, structural, compositional and optical properties. The detailed morphological and structural characterizations revealed that the synthesized nanostructures were flower-shaped, grown in very high-density, and possessed well-crystalline structure. The chemical composition confirmed the presence of Ag into the lattices of Ag-doped ZnO nanoflowers. High sensitivity of $\sim 557.108 \pm 0.012\ mA\ cm^{-2}\ (mol\ L^{-1})^{-1}$ and detection limit of $\sim 5 \times 10^{-9}\ mol\ L^{-1}$ with correlation coefficient (R) of 0.97712 and short response time (10.0 s) were observed for the fabricated chemical sensor towards the detection of phenyl hydrazine by using a simple current–voltage (I–V) technique. Due to high sensitivity and low-detection limit, it can be concluded that Ag-doped ZnO nanoflowers could be an effective candidate for the fabrication of phenyl hydrazine chemical sensors.

1. Introduction

Environmental pollution caused by various means such as automobiles, agricultural run offs and industrial leakages of toxic chemicals and gases at very alarming rate pose a direct threat to human beings and animals by accumulation, entrapment, and suffocation inside their body [1–6]. The leakage of such toxic chemicals contaminates the environment and shows adverse effects to human beings, animals and other living organisms. Among various toxic chemicals, the phenyl hydrazine is one of the most emerging environmental pollutants used in the preparation of pesticides, pharmaceutical, photography chemicals and aerospace fuel. Thus, release of phenyl hydrazine in the environment may cause a severe damage to ecosystem [2–6]. The exposure of this chemical, even at lower concentration, may cause adverse effect to the human body such as skin irritation, dermatitis, hemolytic anemia, liver and kidney injury. In addition to this, phenyl hydrazine is also considered as a carcinogen and thus it is necessary to detect phenyl hydrazine in an effective manner to prevent its side effects towards human and other living organisms [1–6]. There are few reports regarding the determination of phenyl hydrazine through electrochemical techniques where different types of redox mediators were utilized to reduce the high over potential problems in phenyl hydrazine [1–6]. However, these methods lack high sensitivity, good stability and reproducibility. Therefore, a reliable and robust approach for the determination of phenyl hydrazine is still in demand.

Recently, the nanomaterials are utilized as efficient electron mediators for the fabrication of high sensitive chemical and biosensors. Among various nanostructured materials, zinc oxide (ZnO), a II–VI semiconductor material, presents itself as one of the most important functional material with numerous remarkable properties favorable for fabrication of various electronic, optoelectronic, sensors and other nanodevices [1]. The properties which are responsible to make ZnO a multifunctional material are the wide band gap (~3.37 eV), high exciton binding energy (60 meV), biocompatibility, high electron feature and good electrochemical properties, simple and cost effective synthesis, non-toxicity, optical transparency, and so forth [7–20].

* Corresponding authors at: Department of Chemistry, Faculty of Sciences and Arts, Najran University, Najran University, P.O. Box 1988, Najran 11001, Saudi Arabia. Tel.: +966 534 574 597; fax: +966 7 5442 135.
E-mail addresses: shabizaidi79@gmail.com (S.A. Zaidi), ahmadumar786@gmail.com (A. Umar).
[1] Both authors contributed equally in this work.

0039-9140/$ – see front matter © 2012 Elsevier B.V. All rights reserved.
doi:10.1016/j.talanta.2012.02.030

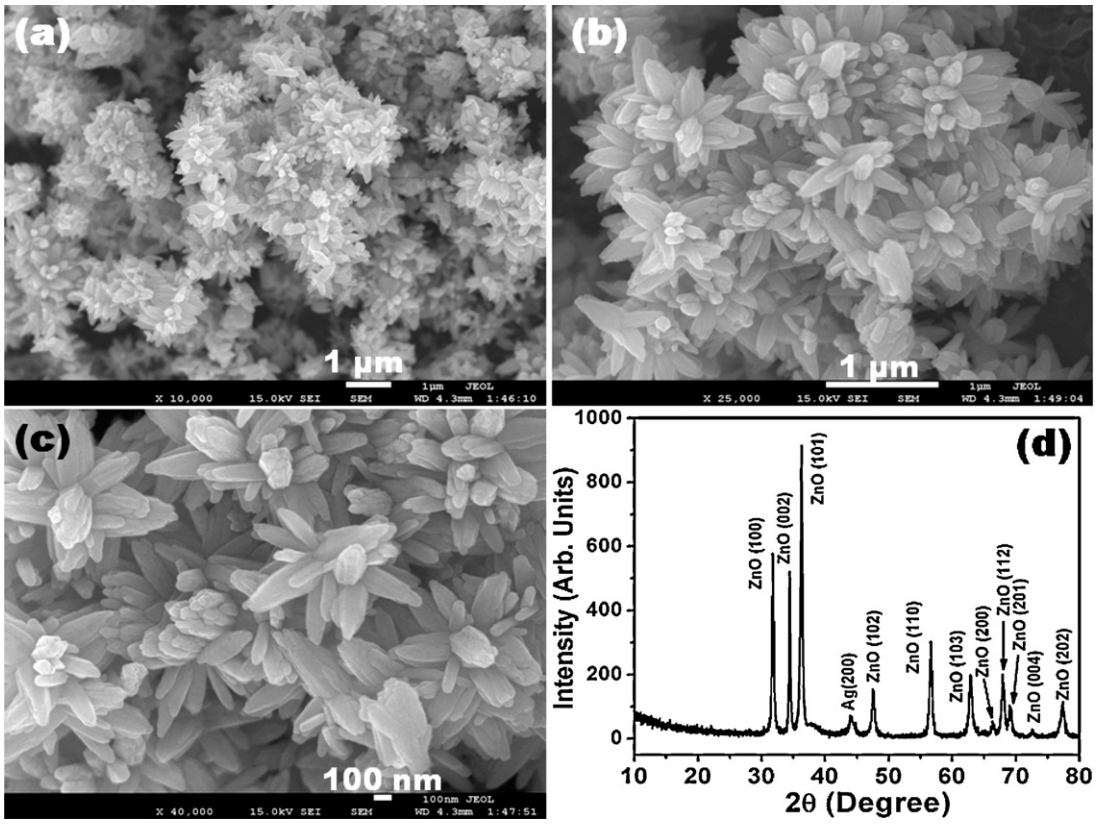

Fig. 1. Low magnification ((a) and (b)) and high-resolution (c) FESEM images and (d) XRD pattern of as-synthesized Ag-doped ZnO nanoflowers.

It is observed that the properties of ZnO nanostructures can be tailored for desired applications through doping, coating and surface modification [10–18]. Therefore, thus far, several metals such as Ga [21], Mn [22], In [23], Mg [24], Al [25], Sb [26], Sn [27], and Ag [28–30] have been utilized to dope the ZnO nanostructures for specific applications and reported in the literature.

Among various metals doped in ZnO nanostructures, the Ag has attracted particular interest due to its various properties. The doping of noble metal (Ag) into semiconductors (ZnO) enhances the optical properties of the resulting nanomaterials [28–30]. Therefore, it was found that the light absorption ability of Ag-doped ZnO thin films was enhanced [31]. In another report, an improved gas sensing property was observed by Ag-doped ZnO nanostructures [30,32]. Even though Ag-doped ZnO possesses excellent properties and have been used in variety of applications, but, to the best of our knowledge, the use of Ag-doped ZnO nanostructures as efficient electron mediator for the fabrication of phenyl hydrazine chemical sensor is not reported yet in the literature.

This research focuses on the fabrication of a phenyl hydrazine chemical sensor based on Ag-doped ZnO nanoflowers. The fabricated chemical sensor showed very high sensitivity and low detection limit. This work offers few important advantages such as facile synthesis of Ag-doped ZnO nanoflowers, simple electrode modification and rapid detection of phenyl hydrazine using the simple current–voltage (*I–V*) technique.

2. Experimental detail

2.1. Synthesis of Ag-doped ZnO nanoflowers

Ag-doped ZnO nanoflowers were synthesized by simple hydrothermal process using zinc nitrate hexahydrate ($Zn(NO_3)_2{\cdot}6H_2O$), silver nitrate ($AgNO_3$) and ammonium hydroxide (NH_4OH) at low-temperature. All the chemicals utilized for the synthesis of Ag-doped ZnO nanoflowers were purchased from Sigma–Aldrich and used as received. To synthesize the Ag-doped ZnO nanoflowers, aqueous solutions of 0.01 mol L^{-1} zinc nitrate and 0.001 mol L^{-1} $AgNO_3$, were mixed under contineous stirrring for 45 min at room-temperature. The pH of the solution was maitained to 9.5 by adding few drops of ammonium hydroxide. The final solution was vigorously stirred for 30 min and consequently transferred to teflon lined autoclave which was then sealed and heated upto 150 °C for 5 h. After terminating the reaction, the autoclave was allowed to cool at room-temperature and the obtained products were washed several times with DI water and ethanol, sequentially and dried at 45 °C. The as-synthesized products were investigated in terms of their morphological, structural, optical and sensing properties.

2.2. Characterization of Ag-doped ZnO nanoflowers

The as-synthesized Ag-doped ZnO nanoflowers were characterized in details using various analytical techniques. Field emission scanning electron microscopy (FESEM; JEOL-JSM-7600F) was used to investigate the general morphologies of as-synthesized nanoflowers. The crystallinity and crystal phases of the as-synthesized nanoflowers were examined by X-ray diffraction (XRD; PANanalytical Xpert Pro.) with Cu-Kα radiation (λ = 1.54178 Å) in the range of 10–80°. The chemical composition was examined by using energy dispersive spectroscopy (EDS), attached with FESEM and Fourier transform infrared (FTIR; Perkin Elmer-FTIR Spectrum-100) spectroscopy in the range of 450–4000 cm^{-1}. UV–visible spectroscopy (Perkin Elmer-UV/VIS-Lambda 950) was done at room-temperature to determine the optical properties of as-synthesized ZnO nanoflowers.

2.3. Fabrication of phenyl hydrazine chemical sensor by using current–voltage (I–V) technique

For the fabrication of phenyl hydrazine sensor, the as-synthesized Ag-doped ZnO nanoflowers were coated on glassy carbon electrode (GCE, surface area 0.0316 cm^2). Before coating, the GC electrode surface was polished with alumina–water slurry on a polishing cloth, followed by thorough rinsing with distilled water. For the electrode surface modification, slurry was made by adding an appropriate composition of Ag-doped ZnO nanoflowers and binder (butyl carbitol acetate). Finally, a certain amount of the slurry was casted on GCE carefully and dried at 60 ± 5 °C for 4–6 h to get a uniform and dry layer over active electrode surface. A simple two electrode system (an electrometer; Keithley, 6517A, USA) was used to evaluate the sensing performance in which the modified electrode was used as working electrode and Pt wire as counter electrode. The current response was measured from 0.0 to +2.0 V while the time delaying and response times were 1.0 and 10.0 s, respectively. The concentration and volume of phosphate buffer solution (PBS) were kept constant to 0.1 mol L^{-1} and 10.0 mL, respectively. A wide concentration range of phenyl hydrazine (1 mol L^{-1} to 10^{-8} mol L^{-1}) was used to check the sensing performance of fabricated phenyl hydrazine chemical sensor.

3. Results and discussion

3.1. Morphological, structural and optical properties of as-synthesized Ag-doped ZnO nanoflowers

The general morphologies of as-synthesized Ag-doped ZnO nanomaterials were investigated by using FESEM and results are shown in Fig. 1(a)–(c). Fig. 1(a) exhibits the typical low-magnification FESEM image, which confirms that the as-synthesized nanomaterials are flower shaped and grown in very high density. The as-synthesized nanoflowers are made up of several triangular-shaped petals and possess sharp tips and wider bases. These wider bases are connected with each other in such a special fashion that they make beautiful flower-like morphologies. The typical diameters at the tips and bases of petals are $\sim 70 \pm 20$ nm and 200 ± 50 nm, respectively. The lengths of petals are in the range of 400–450 nm. The typical dimension of a single flower is $\sim 400 \pm 50$ nm.

To examine the structural properties and crystal phase identifications, powder X-ray diffraction (XRD) was measured with Cu-Kα radiation (λ = 1.54178 Å) in the range of 10–80° with 2°/min scanning speed. The observed XRD pattern exhibits well crystalline nature and mixed phases of Ag and ZnO for as-synthesized nanoflowers (Fig. 1(d)). Several well-defined diffraction reflections related with ZnO were observed in the obtained pattern. The observed diffraction reflections for ZnO (1 0 0), (0 0 2), (1 0 1), (1 0 2), (1 0 3), (2 0 0), (1 1 2), (2 0 1), (0 0 4) and (2 0 2) are similar to bulk ZnO and corresponding to wurtzite hexagonal phase of ZnO. The obtained results are in good agreement with standard JCPDS data card no. 36-1451. In addition to the ZnO reflections, a small peak corresponding to Ag (2 0 0) is also appeared at 44.04°. Except ZnO and Ag, no other reflections related to impurities such as Zn and Ag_2O were found in the pattern.

To check the composition and purity of the as-synthesized Ag-doped ZnO nanoflowers, the nanoflowers were investigated by using energy dispersive spectroscopy (EDS) and elemental mapping, both attached with FESEM, and shown in Figs. 2 and 3, respectively. Fig. 2(a) exhibits the typical FESEM image of as-synthesized Ag-doped ZnO nanoflowers and confirms that the nanoflowers are grown in very high density. To investigate the composition, a selected area of EDS spectrum from Fig. 2(a) has been taken and result is demonstrated in Fig. 2(b). The EDS spectrum shows various well-defined peaks of Zn, O, and Ag. No peak related to any other impurity was detected in the spectrum. This clearly shows that the synthesized nanoflowers are Ag-doped ZnO.

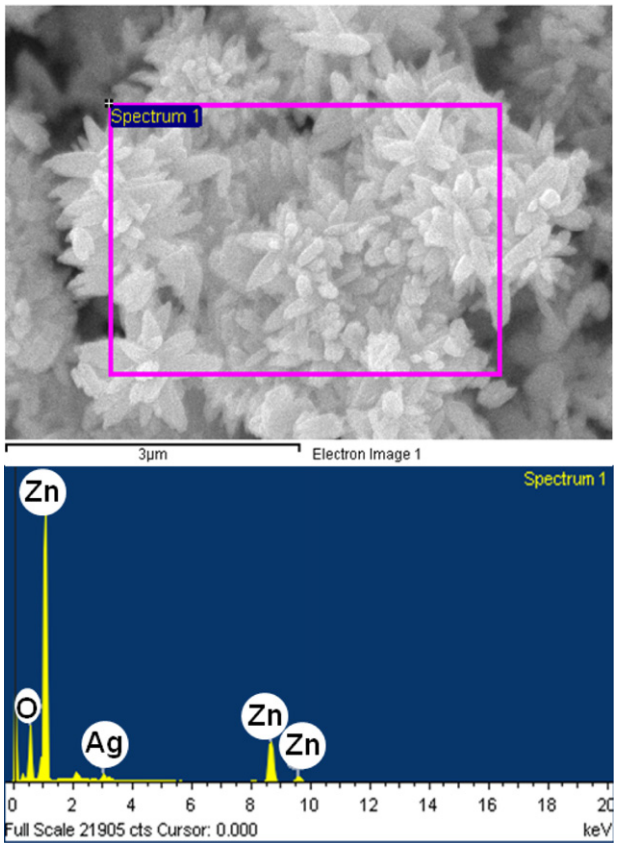

Fig. 2. Typical (a) FESEM image and (b) its corresponding EDS spectrum of as-synthesized Ag-doped ZnO nanoflowers.

It is important to examine the distribution of different ions such as Zn, O and Ag into the lattices of as-synthesized nanoflowers in order to confirm that the substituted metal is distributed homogeneously over the whole crystal. Fig. 3(a) exhibits the typical FESEM image of as-synthesized Ag-doped ZnO nanoflowers while the Fig. 3(b)–(d) depict the corresponding elemental mapping (elemental distribution along the whole crystal) for Zn, O and Ag. It is evident from Fig. 3(b)–(d) that the number of spots corresponding to Zn and O are higher in density and the homogenous distribution of Zn and O is evident (Fig. 3(b) and (c)). The smaller number of spots for Ag as compared to those for Zn and O are due to the less amount of Ag metal doping into the lattices of as-synthesized nanoflowers (Fig. 3(d)). Thus, the elemental mapping further confirmed that the synthesized nanoflowers are Ag-doped ZnO.

The quality and chemical composition of as-synthesized Ag-doped ZnO nanoflowers were investigated by FTIR spectroscopy at room-temperature in the range of 450–4000 cm^{-1} and demonstrated in Fig. 4. Several absorption peaks at 481, 891, 1382, 1623 and 3425 cm^{-1} were observed in the obtained FTIR spectrum. The absorption peak appeared at about 481 cm^{-1} is related to a typical FTIR absorption peak of ZnO which originates from stretching mode of the Zn—O bond [10,33,34]. Two very small peaks originated at ~891 cm^{-1} and ~1382 cm^{-1} are probably due to the nitrate (NO_3^-) groups [35,36]. Appearance of another small absorption peak at 1623 cm^{-1} could be ascribed to the bending vibration of absorbed water and surface hydroxyl [37]. Furthermore, a well-defined absorption peak appeared at 3425 cm^{-1} is related to the O—H stretching mode [37]. Except above mentioned absorption

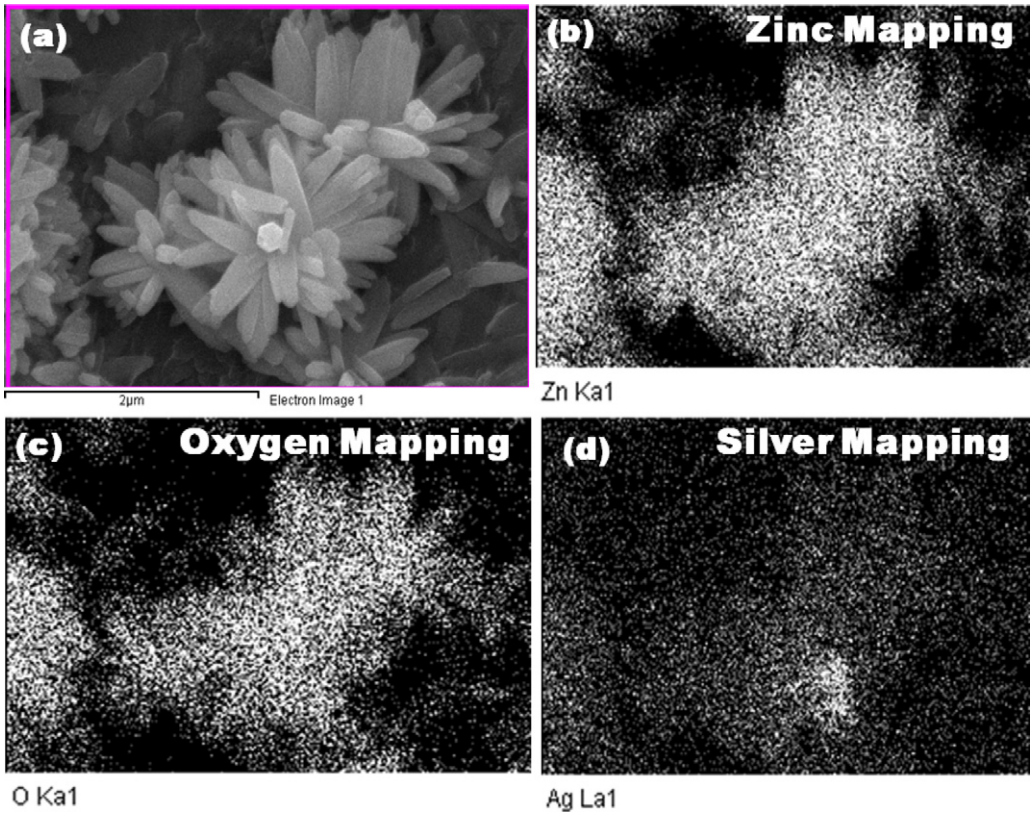

Fig. 3. Typical (a) FESEM image and its corresponding elemental mapping images for (b) zinc, (c) oxygen and (d) silver of as-synthesized Ag-doped ZnO nanoflowers.

bands, no other distinguished peak related to any other functional group is detected in the FTIR spectrum which clearly reflects that the synthesized product is without any significant impurity.

UV–vis spectroscopy was performed to examine the optical property of as-synthesized Ag-doped ZnO nanoflowers at room-temperature and result is reported in Fig. 5. The as-synthesized Ag-doped ZnO nanoflowers exhibit a single and well-defined absorption band at 377 nm, which is the characteristic band for the wurtzite hexagonal structure of ZnO [38]. The obtained UV–vis spectrum for Ag-doped ZnO nanoflowers does not show any significant change in the absorption spectrum due to the doping of Ag into ZnO lattices. The observed results are almost similar with the already reported literature [39].

3.2. Phenyl hydrazine chemical sensor application of as-synthesized Ag-doped ZnO nanoflowers

The methodology for the detection of phenyl hydrazine using the typical current–voltage (*I–V*) technique has been extensively described in the experimental detail section. In short, slurry of as-grown Ag-doped ZnO mixed with certain amount of binder was casted on GC electrode and dried. In two electrode *I–V* system, the modified GCE was used as working electrode while Pt wire was employed as a counter electrode. The current response was measured from 0.0 to +2.0 V and the time delaying and response times were 1.0 and 10.0 s, respectively.

The schematic for the fabrication of Ag-doped ZnO nanoflowers based phenyl hydrazine chemical sensor and its mechanism have

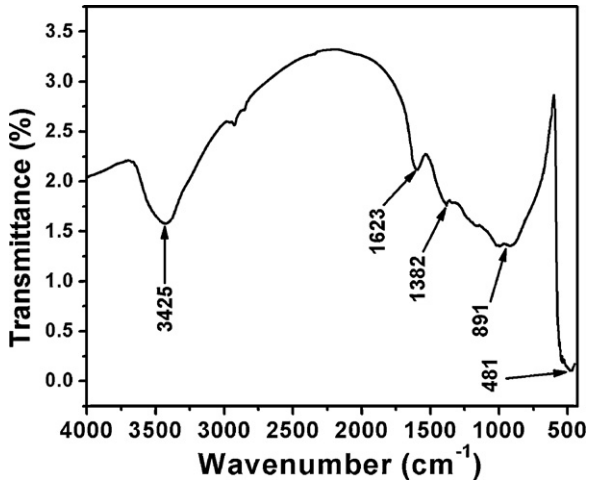

Fig. 4. FTIR spectrum of as-synthesized Ag-doped ZnO nanoflowers.

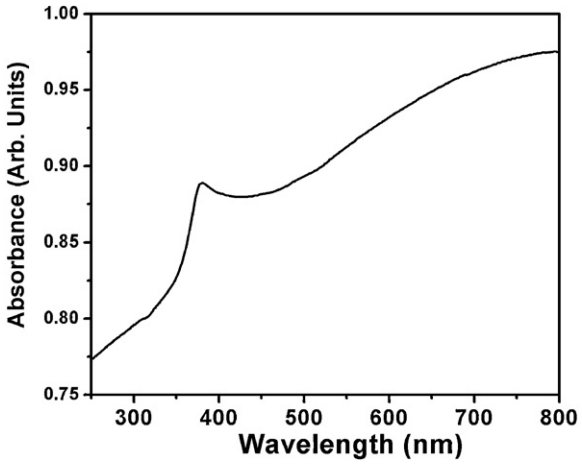

Fig. 5. UV–vis spectrum of as-synthesized Ag-doped ZnO nanoflowers.

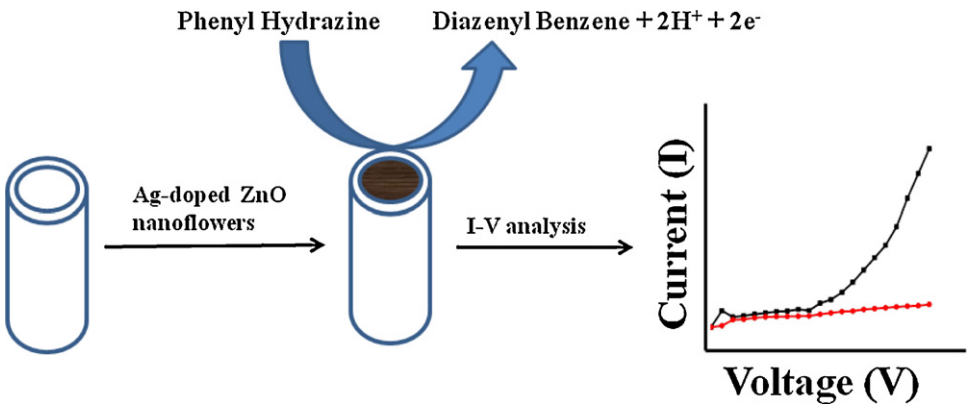

Fig. 6. Schematic representation of phenyl hydrazine chemical sensor fabrication based on Ag-doped ZnO nanoflowers coated GCE electrode and its sensing mechanism by simple and facile *I–V* technique.

been illustrated in Fig. 6. The proposed Ag-doped ZnO nanoflowers modified sensor was applied to detect phenyl hydrazine in liquid phase. The detection of phenyl hydrazine with this modified sensor is typically attributed to the oxidation and reduction properties of metal oxides nanostructures (Ag-doped ZnO in the present case). The oxygen is very essential part of the sensing mechanism and the adsorption of the oxygen at nanomaterial surface depends on the structural properties of doped material. Firstly, the oxygen is adsorbed chemically at liquid surface boundary while the physiosorption of oxygen monolayer takes place at Ag-doped ZnO nanomaterial surface from the bulk solution. The number of defects in the Ag-doped ZnO nanomaterial surface, due to doped metal, enhance the oxygen adsorption. It is also known that oxidizing behavior of nanomaterial is increased due to increase in the amount of adsorbed oxygen. The oxygen which takes part in the detection procedure is subsequently converted into dynamic oxygen species i.e. O_2^- and O^- depending on the available energy bands after extracting the electrons from Ag-doped ZnO nanoflowers surface. These procedures occur according to following reactions (1) and (2).

$$2O_{2(g)} \rightarrow 2O_{2(ads)} \quad (1)$$

$$O_{2(ads)} + 2e^-(\text{Ag-dopedZnO}) \rightarrow 2O^-_{(ads)}(O^-/O_2^-) \quad (2)$$

The emission of the electrons according to reaction (2) decreases the conductance properties and increases the resistance of Ag-doped ZnO nanoflowers, thus, creating the holes for conduction that play pivotal role in phenyl hydrazine sensing. Due to the decrease in conductance, the value of current is reduced. In second step, the phenyl hydrazine is oxidized to diazenyl benzene in the presence of dynamic oxygen species and emits two free electrons simultaneously as shown in reaction (3).

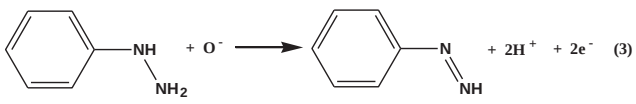

(3)

According to reaction (3), the oxygen ions are consumed and the doped nanoflowers surface captures the released electrons, consequently the conducting behavior of doped nanomaterial surface is amplified [40].

The current responses of the sensor with and without coating of Ag-doped ZnO nanoflowers material over GCE are shown in Fig. 7. The lower current value was observed with nanomaterial modified GCE compared to non-modified (no coating) GCE in 0.1 mol L^{-1} PBS buffer. The decrease in current response may be due to the increase in the surface resistance of modified electrode surface. To observe the sensor behavior in different concentration of phenyl hydrazine solutions, the *I–V* signals were measured. This is clear from Fig. 8(a) that the value of current increases substantially from lower to higher concentrations (10^{-8} mol L^{-1} to 1 mol L^{-1}) of phenyl hydrazine. The reason of observed current behavior lies in the fact that the ionic strength of the solution was increased by increasing the phenyl hydrazine concentration, thus producing more number of ions.

The sensitivity of the fabricated phenyl hydrazine chemical sensor was acquired by the slope of the current–concentration calibration profile. The sensitivity was obtained when the slope was divided by the active surface area of electrode according to the equation: "Sensitivity = Slope/Surface area of electrode" (surface area of GCE is 0.0316 cm^2). The calibration curve was plotted by taking average of currents over a range of potentials spanning from 0.5 to 1.1 V. The calibration data was fitted well linearly at smaller scale concentration range (10^{-8} mol L^{-1} to 10^{-3} mol L^{-1}), from which the slope was calculated. The calibration (sensitivity) curve of the fabricated sensor is shown in Fig. 8(b). According to the calibration curve, the calculated sensitivity of the fabricated phenyl hydrazine chemical sensor was found

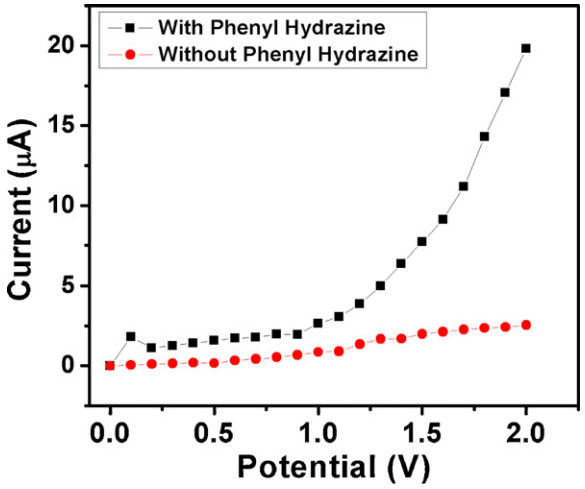

Fig. 7. Typical *I–V* response of glassy carbon electrode (GCE) in 10 ml, 0.1 M PBS solution: (■) with 10^{-8} mol L^{-1} phenyl hydrazine and (●) without the presence of phenyl hydrazine.

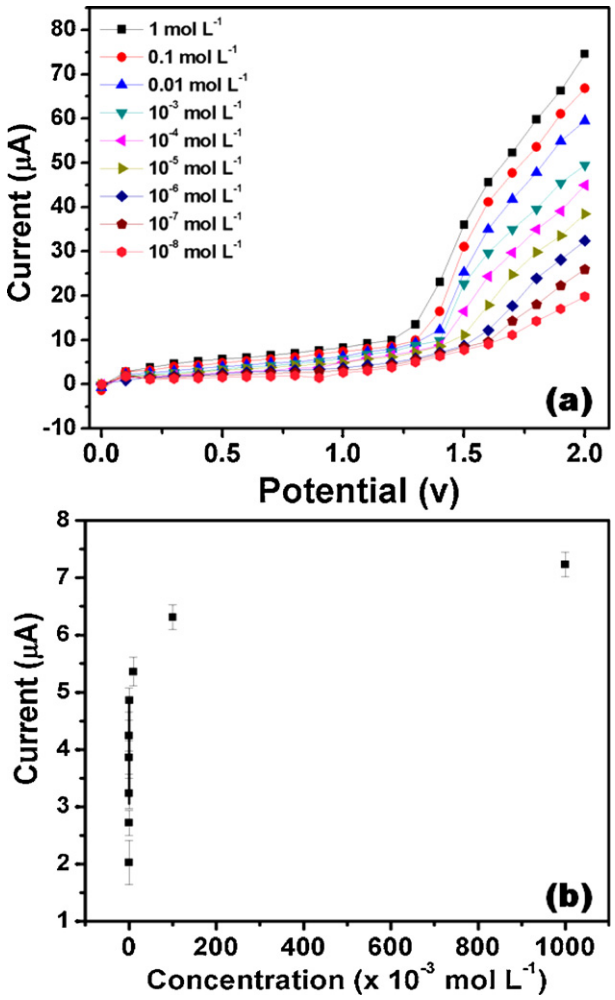

Fig. 8. (a) Typical *I–V* response of Ag-doped ZnO nanoflowers modified GCE towards various concentrations (from 10^{-8} mol L^{-1} to 1 mol L^{-1}) of phenyl hydrazine into 0.1 M PBS solution (pH = 7) and (b) calibration curve.

to be $\sim 557.108 \pm 0.012$ mA cm^{-2} (mol $L^{-1})^{-1}$. The observed sensitivity of the fabricated chemical sensor is higher than the fabricated phenyl hydrazine sensor based on modified carbon paste electrode [2]. The detection limit of the fabricated phenyl hydrazine sensor was determined to be $\sim 5 \times 10^{-9}$ mol L^{-1} which is lower than previously fabricated phenyl hydrazine chemical sensors based on modified carbon paste electrode [2], lectin glycoenzyme multilayer film modified sensor [4], horseradish peroxidase (HRP) inhibition biosensor for determination of phenyl hydrazine [5] and ferrocene-carbon nanotubes modified carbon paste electrode [6]. The correlation coefficient (R) of the fabricated chemical sensor was found to be ~0.97712 and the current exhibited the linearity in the range of 10^{-8} mol L^{-1} to 10^{-3} mol L^{-1}.

The proposed phenyl hydrazine chemical sensor showed good stability and reproducibility. The stability of the present phenyl hydrazine sensor was determined by the repetitive measurements once a day for 5 weeks. After each measurement, the sensor was stored in a phosphate buffer solution (pH = 7.0). No significant decrease in phenyl hydrazine detection was observed for 5 weeks. After 5 weeks, the response of sensor was gradually reduced due to the weak interaction of phenyl hydrazine and nanomaterial surface.

4. Conclusion

In summary, a robust, highly sensitive, reliable and reproducible phenyl hydrazine chemical sensor was fabricated by utilizing simply synthesized Ag-doped ZnO nanoflowers as efficient electron mediator. The as-synthesized nanoflowers were characterized in terms of their structural and optical properties which revealed the well-crystalline nature and good optical properties for as-synthesized products. A very high sensitivity of $\sim 557.108 \pm 0.012$ mA cm^{-2} (mol $L^{-1})^{-1}$ and detection limit of $\sim 5 \times 10^{-9}$ mol L^{-1} with a correlation coefficient (R) of 0.97712 and less response time of 10 s were observed for the fabricated chemical sensor towards the detection of phenyl hydrazine by simple current–voltage (*I–V*) technique. This research opens a way that simply synthesized Ag-doped ZnO nanomaterials could be used as efficient electron mediators for the fabrication of various effective chemical sensors.

Acknowledgements

Authors would like to acknowledge the support of the Ministry of Higher Education, Saudi Arabia for this research through a grant for a Promising Centre on Sensors and Electronic Devices at Najran University, Saudi Arabia, dated 24/3/1432 H, 27/02/2011. Ahmad Umar also greatly acknowledges the financial support of Deanship of Scientific Research (Project Grant no. NU/27/11), Najran University, Najran, Saudi Arabia. AU, GND and SAZ also greatly acknowledge the Promising Centre for Sensors and Electronic Devices Project (PCSED-001-11).

References

[1] A. Umar, Y.B. Hahn (Eds.), Metal Oxide Nanostructures and their Applications, Part IV, American Scientific Publisher, USA, 2010.
[2] N. Rastakhiz, A. Kariminik, V.S. Nejad, S. Roodsaz, Int. J. Electrochem. Sci. 5 (2010) 1203–1212.
[3] S. Chitravathi, B.E. Kumara Swamy, U. Chandra, G.P. Mamatha, B.S. Sherigara, J. Electroanal. Chem. 645 (2010) 10–15.
[4] L. Tang, G.M. Zeng, Y.H. Yang, G.L. Shen, G.H. Huang, C.G. Niu, W. Sun, J.B. Li, Int. J. Environ. Anal. Chem. 85 (2005) 111–125.
[5] Z.S. Yang, W.L. Wu, X. Chen, Y.C. Liu, Anal. Sci. 24 (2008) 895–899.
[6] D. Afzali, H.K. Maleh, M.A. Khalilzadeh, Environ. Chem. Lett. 9 (2010) 375–381.
[7] L. Schmidt-Mende, J.L. MacManus-Driscoll, Mater. Today 10 (2007) 40–48.
[8] A. Umar, M.M. Rahman, S.H. Kim, Y.B. Hahn, Chem. Commun. 2 (2008) 166–168.
[9] R. Wahab, Y.S. Kim, D.S. Lee, J.M. Seo, H.S. Shin, Sci. Adv. Mater. 2 (2010) 35–42.
[10] J. Wu, D. Xue, Sci. Adv. Mater. 3 (2011) 127–149.
[11] S.G. Ansari, Z.A. Ansari, R. Wahab, Y.S. Kim, G. Khang, H.S. Shin, Biosens. Bioelectron. 23 (2008) 1838–1842.
[12] P. Gouma, Sci. Adv. Mater. 3 (2011) 787–793.
[13] G.N. Dar, A. Umar, S.A. Zaidi, S. Baskoutas, S.W. Hwang, M. Abaker, A. Al-Hajry, S.A. Al-Sayari, Talanta 89 (2012) 155–161.
[14] K.I. Choi, J.H. Lee, Sci. Adv. Mater. 3 (2011) 811–820.
[15] A. Khan, S.N. Khan, W.M. Jadwisienczak, Sci. Adv. Mater. 2 (2010) 572–577.
[16] B. Haghighi, S. Bozorgzadeh, Talanta 85 (2011) 2189–2193.
[17] H. Zeng, J. Cui, B. Cao, U. Gibson, Y. Bando, D. Golberg, Sci. Adv. Mater. 2 (2010) 336–358.
[18] Z. Zhang, Y. Yuan, Y. Fang, L. Liang, H. Ding, L. Jin, Talanta 73 (2007) 523–528.
[19] R. Ding, J. Liu, J. Jiang, X. Ji, X. Li, F. Wu, X. Huang, Sci. Adv. Mater. 2 (2010) 396–401.
[20] S.K. Mohanta, D.C. Kim, B.H. Kong, H.K. Cho, W. Liu, S. Tripathy, Sci. Adv. Mater. 2 (2010) 64–68.
[21] J. Zhong, S. Muthukumar, Y. Chen, Y. Lu, H.M. Ng, E.L. Garfunkel, Appl. Phys. Lett. 83 (2003) 3401–3403.
[22] C. Ronning, P.X. Gao, Y. Ding, Z.L. Wang, D. Schwen, Appl. Phys. Lett. 84 (2004) 783–785.
[23] J.S. Jie, G.Z. Wang, X.H. Han, Q.X. Yu, Y. Liao, G.P. Li, J.G. Hou, Chem. Phys. Lett. 387 (2004) 466–470.
[24] L.P. Zhu, M.J. Zhi, Z.Z. Ye, B.H. Zhao, Appl. Phys. Lett. 88 (2006) 113106–113113.
[25] R.C. Wang, C.P. Liu, J.L. Huang, S.J. Chen, Appl. Phys. Lett. 88 (2006) 023111–23113.
[26] S.H. Kim, A. Umar, Y.K. Park, J.H. Kim, E.W. Lee, Y.B. Hahn, J. Alloys Compds. 479 (2009) 290–293.
[27] H. Chen, J. Qi, Y. Huang, Q. Liao, Y. Zhang, Acta Phys. Chim. Sin. 23 (2007) 55.
[28] S. Liu, C. Li, J. Yu, Q. Xiang, Cryst. Eng. Commun. 13 (2011) 2533–2541.
[29] Y. Lai, M. Meng, Y. Yu, Appl. Catal. B: Environ. 100 (2010) 491–501.
[30] X. Li, Y. Wang, J. Alloys Compds. 509 (2011) 5765–5768.

[31] S.W. Dian, W.Y. Lian, Chin. J. Vac. Sci. Technol. 27 (2007) 309–311.
[32] F.X. Hui, L. He, M.X. Hong, Y. Wen, Nanosci. Nanotechnol. 6 (2009) 61–65.
[33] R. Chakravarty, C. Periasamy, Sci. Adv. Mater. 3 (2011) 276–283.
[34] L.S. Roselin, R. Selvin, Sci. Adv. Mater. 3 (2011) 251–258.
[35] Y.H. Ni, X.W. Wei, J.M. Hong, Y. Ye, Mater. Sci. Eng. B 121 (2005) 42–47.
[36] M.S. Chauhan, R. Kumar, A. Umar, S. Chauhan, G. Kumar, S.W. Hwang, A. Al-Hajry, J. Nanosci. Nanotechnol. 11 (2011) 4061–4066.
[37] R.A. Nyquist, R.O. Kagel, Infrared Spectra of Inorganic Compounds, Academic Press, Inc., New York, London, 1971.
[38] A. Al-Hajry, A. Umar, Y.B. Hahn, D.H. Kim, Superlatt. Microstruct. 45 (2009) 529–534.
[39] C. Ren, B. Yang, M. Wu, J. Xu, Z. Fu, Y. lv, T. Guo, Y. Zhao, C. Zhu, J. Hazard. Mater. 182 (2010) 123–129.
[40] S. Majumdar, Mater. Sci. Poland 27 (2009) 123–129.